

Genetic Algorithms to Automate the Design of Metasurfaces for Absorption Bandwidth Broadening

Junming Zhang, Guowu Wang, Tao Wang,* and Fashen Li



Cite This: *ACS Appl. Mater. Interfaces* 2021, 13, 7792–7800



Read Online

ACCESS |

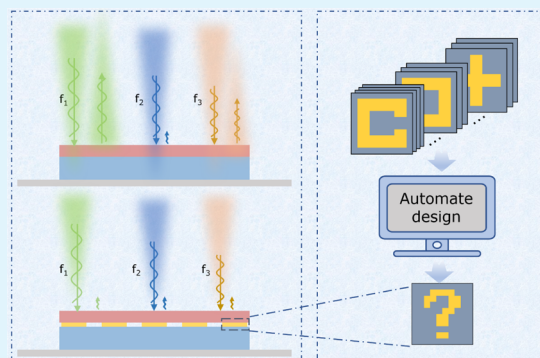
Metrics & More

Article Recommendations

Supporting Information

ABSTRACT: In this paper, we present a method to automate the design of an efficient metasurface, which widens the bandwidth of the substrate. This strategy maximizes the potential of the substrate for the application of broad-band absorption. The design is achieved by utilizing the coding metasurface and a combination of two types of intelligent algorithms. First, inspired by the coding metasurface, a large number of structures are generated to act as potential metasurface unit patterns by randomly generating the associated binary codes. Then, the binary codes are directly substituted as optimization objects into a genetic algorithm to find the optimal metasurface. Finally, a neural network is introduced to replace the finite element analysis method to correlate the binary codes with the absorbing bandwidth. With the participation of neural networks, the genetic algorithm can find the optimal solution in a considerably short time. This method bypassed the prerequisite physical knowledge required in the process of metasurface design, which can be used for reference in other applications of the metasurface.

KEYWORDS: metasurfaces, broad-band absorption, neural networks, genetic algorithms, design strategy



1. INTRODUCTION

Microwave-absorbing materials are one of the most important functional materials in recent decades.^{1–4} Initially, they were mainly used to avoid radar detection of military equipment.⁵ In recent years, the rapid development of microwave technology has led to the proliferation of a large number of commercial devices, such as mobile phones⁶ and antennas,⁷ which need to be protected from the influence of external electromagnetic waves. Microwave-absorbing materials are more commonly used for this purpose. With the increase in application scenarios, there is a high demand for microwave-absorbing materials with a broader absorption bandwidth. However, at present, the working band of conventional microwave-absorbing materials is relatively narrow.^{8–11} To meet the higher demand, the bandwidth of the conventional absorber should be broadened. Many methods have been reported to solve this issue.^{12–15} In one of the popular methods, a metasurface is loaded on a conventional absorber substrate. This method significantly improves the absorption bandwidth.^{16–18} In addition, as the metasurface is extremely thin and light, combining the metasurface with the conventional absorbing substrate will not affect the original thickness. This is a distinct advantage that no other approaches have, so that attracts a lot of attention.

A metasurface can expand the absorbing bandwidth only if it matches with the absorber substrate. Hence, researchers have developed different design strategies based on the substrate's

intrinsic properties and corresponding physical mechanisms. For example, Fan et al. used a high-loss material as a substrate and designed a phase gradient metasurface to broaden the bandwidth.¹⁹ They designed a metasurface that changed the propagation direction of the incident wave, which led to an increase in the propagation distance inside the substrate. The longer propagation distance results in increased energy attenuation in different frequencies, thus eventually expanding the absorbing band. Duan et al. also chose a high-loss material as the substrate,¹⁵ which showed a good absorption performance in a narrow band due to the destructive interference mechanism. They designed a metasurface to adjust the intensity of the separated waves reflected by different interfaces at different frequencies. This improved the interference canceling at different frequencies and expanded the absorbing band. Xu et al. chose a lossless material as the substrate.²⁰ In their work, the substrate was not used to absorb the incident wave. Instead, the substrate provided an environment matching the designed metasurface, which allowed the scattering of the vertical incident wave in the horizontal

Received: December 14, 2020

Accepted: January 26, 2021

Published: February 3, 2021



ACS Publications

© 2021 American Chemical Society

7792

<https://dx.doi.org/10.1021/acsami.0c21984>
ACS Appl. Mater. Interfaces 2021, 13, 7792–7800

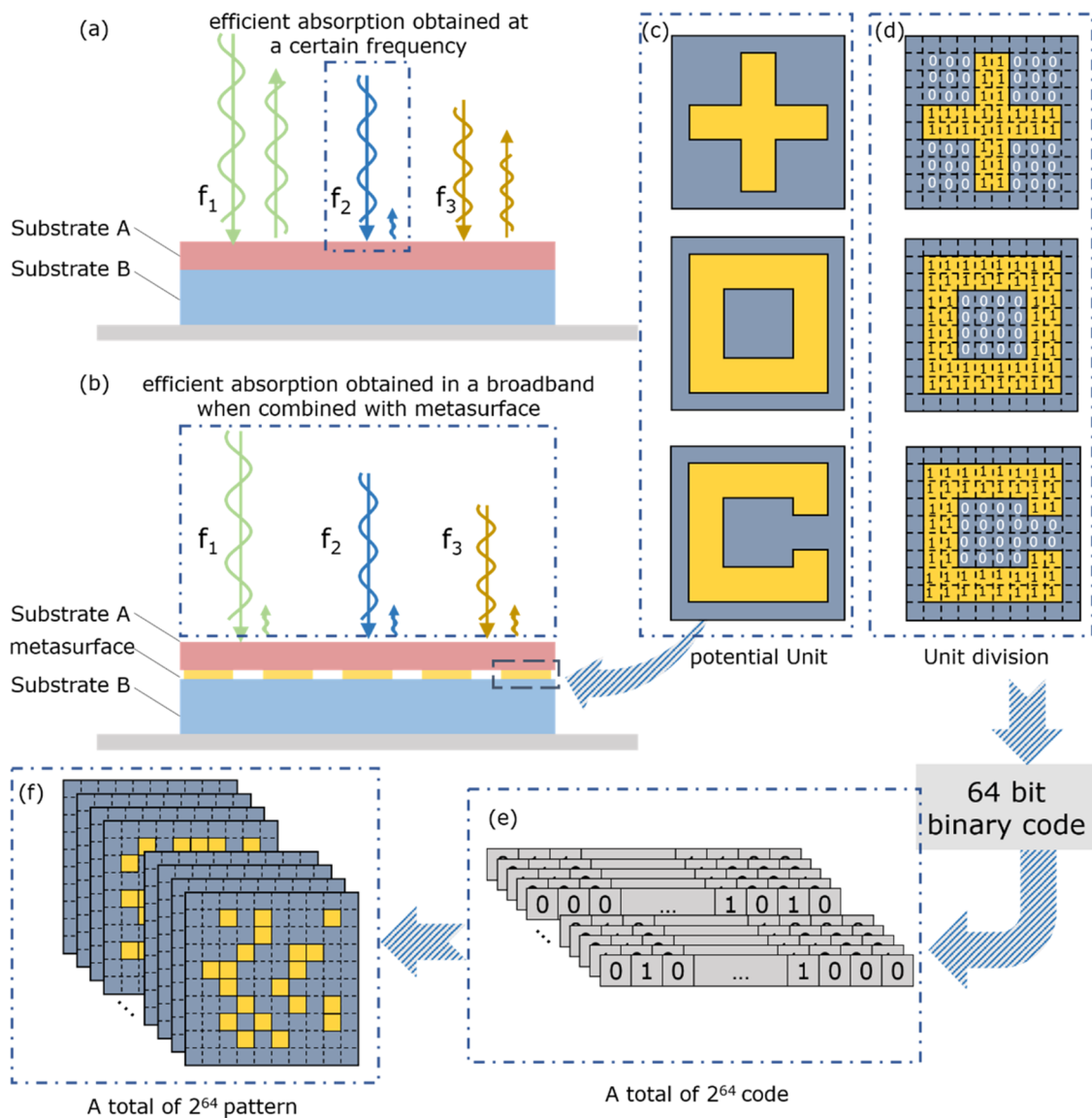


Figure 1. (a) Schematic of a narrow band conventional absorber. (b) Schematic of a wideband metamaterial absorber composed of a metasurface and a conventional absorbing substrate. (c) Potential structure design of a metasurface pattern unit. (d) Schematic of array unit coding. (e) Division of the array pattern into 2^{64} binary codes corresponding to an 8×8 grid. (f) Total of 2^{64} possible array patterns.

direction. The direction change avoided the detection of the wave, thus improving the absorbing band.

Though the aforementioned methods have improved the absorbing band, they have some common drawbacks. First, the performance of the designed metasurface greatly depends on the intrinsic characteristics of the substrate material. If the substrate material is changed after fixing the metasurface design, the design will not maintain its original function and the original design strategy may also fail. Till date, there is no universal design strategy for metasurfaces. Second, though the metasurfaces designed by these methods affect the bandwidth of the substrate, it is not clear if the design of the metasurface allows the substrate to achieve its full broad-band absorption potential. This issue has been rarely studied. Third, the design of a metasurface requires not only a solid physical foundation but also a clear understanding of the intrinsic properties of the different substrates, which requires knowledge from different subjects. Hence, a simple and efficient design strategy is required to promote the widespread use of metasurfaces.

Here, we present a method to design metasurfaces that can be used to broaden the absorption bandwidth of different substrate materials. The method realizes the automatic design of a bandwidth expansion metasurface, which can be achieved without the physical knowledge required in the traditional design strategy. Most importantly, **the proposed design technique can maximize the potential of the substrate in the application of broad-band absorption**. The metasurface designed by this method can be approximately regarded as the global optimal solution. We call it **automated bandwidth expansion design (Auto-BED)**. To realize these functions, in the first step of this system, referred to as the “coding metasurface”,²¹ we meshed and coded the metasurface so that a large number of different metasurface patterns can be generated by generating different codes. As the codes correspond to the metasurface array, which, in turn, corresponds to the absorbing performance, the optimal performance can be achieved by optimizing the codes. **This process of code optimization is based on the finite element**

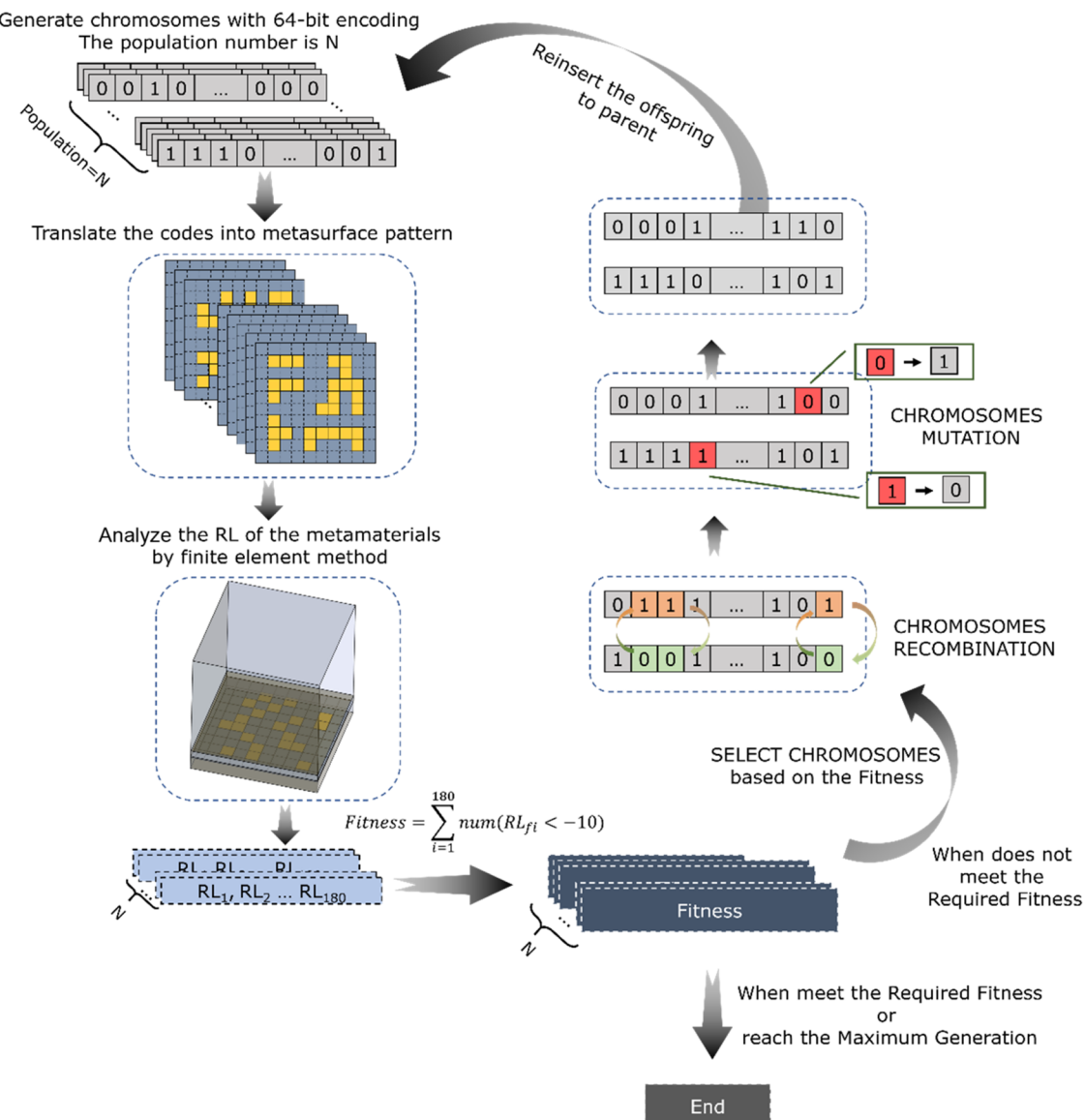


Figure 2. Flow chart of the genetic algorithm for the generation of the optimal metasurface.

method associated with a genetic algorithm,^{22,23} in which the finite element method is mainly used to calculate the absorbing performance of metamaterial absorbers with different metasurface patterns, and the genetic algorithm is used to select the optimal solution efficiently. To further reduce the time consumed during this process, the finite element method, which requires a long time to simulate the absorbing performance, is replaced by a neural network.²⁴ With the trained neural network as the link to connect the metasurface pattern and the corresponding absorption performance, the genetic algorithm can work more quickly to select the best-matched codes, i.e., the metasurface arrays. As an example, in this paper, a common substrate was selected. Its most matched metasurface was picked out by the above method. The simulation results are in good agreement with the experimental results.

2. CODING METASURFACES

The metasurface is compounded with a substrate material to achieve a broader bandwidth, as shown in Figure 1a,b (magnetic substrates were used here as an example, and

details on them can be found in the Supporting Information). In the conventional design method, the unit structure of the metasurface is generally determined first, as shown in Figure 1c. Then, by optimizing the geometric parameters of the structure, the optimal solution is selected.^{25–27} The optimization process of geometric parameters can be carried out directly with the built-in program of the high-frequency structure simulator (HFSS). However, the built-in optimization of the software can only target the geometric parameters without changing the structure pattern of the metasurface unit. The results obtained by this method can only be regarded as the local optimal solution. To obtain the global optimal solution, it is necessary not only to study the effect of different geometric parameters but also to investigate the results in different pattern structures. Hence, a large number of different unit structures are required to obtain the global optimal metasurface.

This requirement can be satisfied by coding the metasurface.^{21,28–30} As shown in Figure 1d, the metasurface unit cell is uniformly divided into n^2 lattices (as an example, in this study, the length of the unit cell is 2 mm and the unit is divided into

64 lattices). A lattice with a copper covering is marked as 1; other lattices are marked as 0. In this way, by encoding all of the lattice points, the metasurface structure corresponds to a set of 64-bit binary codes. In other words, a pattern can be generated by randomly generating 64-bit binary codes. Using the network partitioning method in this article as an example, 2^{64} patterns are generated directly.

However, the generation of a huge amount of structures poses another problem that makes further operation difficult. The process of listing all of the geometries, calculating their absorbing performance, and finding the optimal structure is computationally intensive because of the amount of data. It is necessary to reduce the number of calculations to find the optimal structure. In this study, a genetic algorithm is used for this purpose.

3. GENETIC ALGORITHM

A genetic algorithm is an intelligent algorithm that simulates the natural selection process of Darwinian biological evolution. It is a computational model of the biological evolution process of genetic mechanisms, which searches for the optimal solution by simulating the natural evolution process. In this algorithm, the data are first organized as a population of many individuals with different chromosomes. The individuals are judged on their suitability to the environment, which is labeled as their “fitness,” by means of a threshold. The more adaptable an individual is, the more chances it has to pass on its chromosomes to the next generation. The operations of selection, crossover, and mutation are processed to generate individuals with new chromosomes. After many rounds, the best-adapted individuals are generated.

A schematic of the genetic algorithm for choosing metasurfaces is shown in Figure 2. Here, the metasurface pattern is the optimized object. The individual of the population in the genetic algorithm is the array unit structure. Since the structure has been encoded, the 64-bit binary code can be directly used as the individual chromosome for subsequent operations. The broad-band absorption is chosen as the evaluation criteria in this paper, and hence the absorption bandwidth is set as environment suitability, i.e., the fitness. In this process, HFSS is used to obtain the absorbing performance at different frequencies. The absorption bandwidth can be represented and the fitness function can be defined by counting the number of frequency points of reflection loss (RL) less than -10 dB. The individuals in the initial population that meet the fitness criteria are selected and their chromosomes (i.e., the 64-bit code) undergo the crossover and mutation operation. Eventually, individuals with new chromosomes are generated. These individuals are then inserted back into the original population to replace individuals with low fitness. The entire process is repeated until the fitness remains unchanged or the set maximum cycle is reached. At this step, the individual with the strongest adaptability is picked out, which corresponds to the best-matched metasurface pattern.

As the genetic algorithm does not go through all of the possibilities to pick out the best result, the computational time taken is greatly reduced. However, even though it is not necessary to traverse every possibility, a large number of individuals and a large number of cycles are required during the operation of the genetic algorithm to ensure reliable results. Assuming that the number of individuals in the population is 10 000 and the maximum genetic algebra is 100,

the entire process still needs to simulate the absorbing performance 10^6 times. Another important point is that the process mentioned above calls HFSS to simulate the results. Even if a script is used for modeling in the software,^{31,32} it takes approximately 3 min to process a single sample. Considering that there are 10^6 samples, this program will take about 69 months in total to reach completion. Spending this amount of computational time for the bandwidth expansion optimization of a single kind of substrate material is clearly not practical. The time consumed in this step has to be reduced significantly to achieve efficient operation.

4. ARTIFICIAL NEURAL NETWORKS

There is currently no analytical solution for the complex pattern designs shown in this paper. The only solution is to simulate the results by full-wave analysis software. During the implementation of the genetic algorithm, HFSS needs to be called repeatedly to obtain the corresponding absorbing performance of different metasurfaces. However, the calculation process of HFSS is cumbersome and time-consuming. The entire process is shown in Figure 3. It is necessary to first

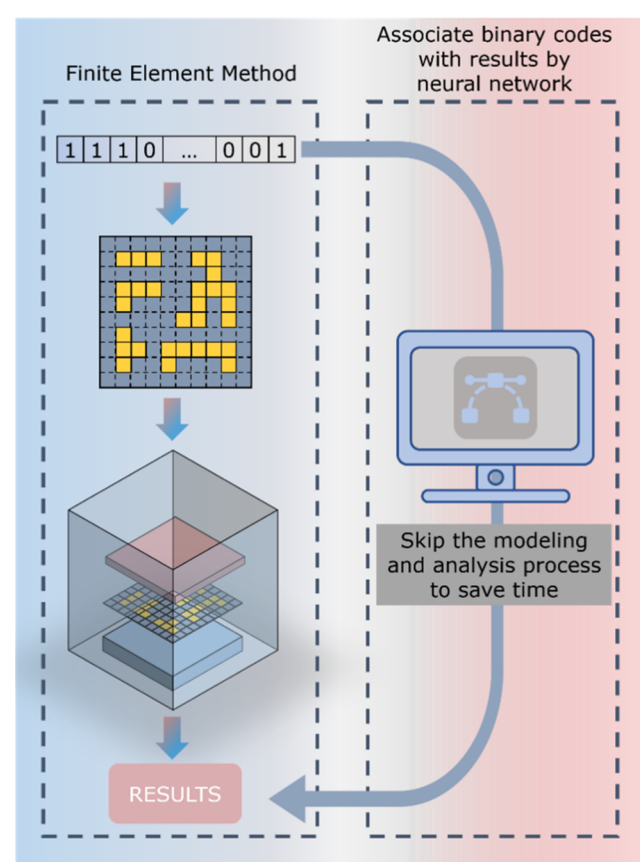


Figure 3. Schematic showing the calculation of the absorption performance by HFSS and the same process using a neural network.

transfer the codes to a structure, followed by modeling this structure in HFSS, and finally analyzing its performance. If a function that connects the codes and absorption performance is found, the time consumed in this process will be greatly shortened.²⁴ Here, we trained a neural network to solve this problem.

An artificial neural network is a mathematical model of distributed parallel information processing that imitates the

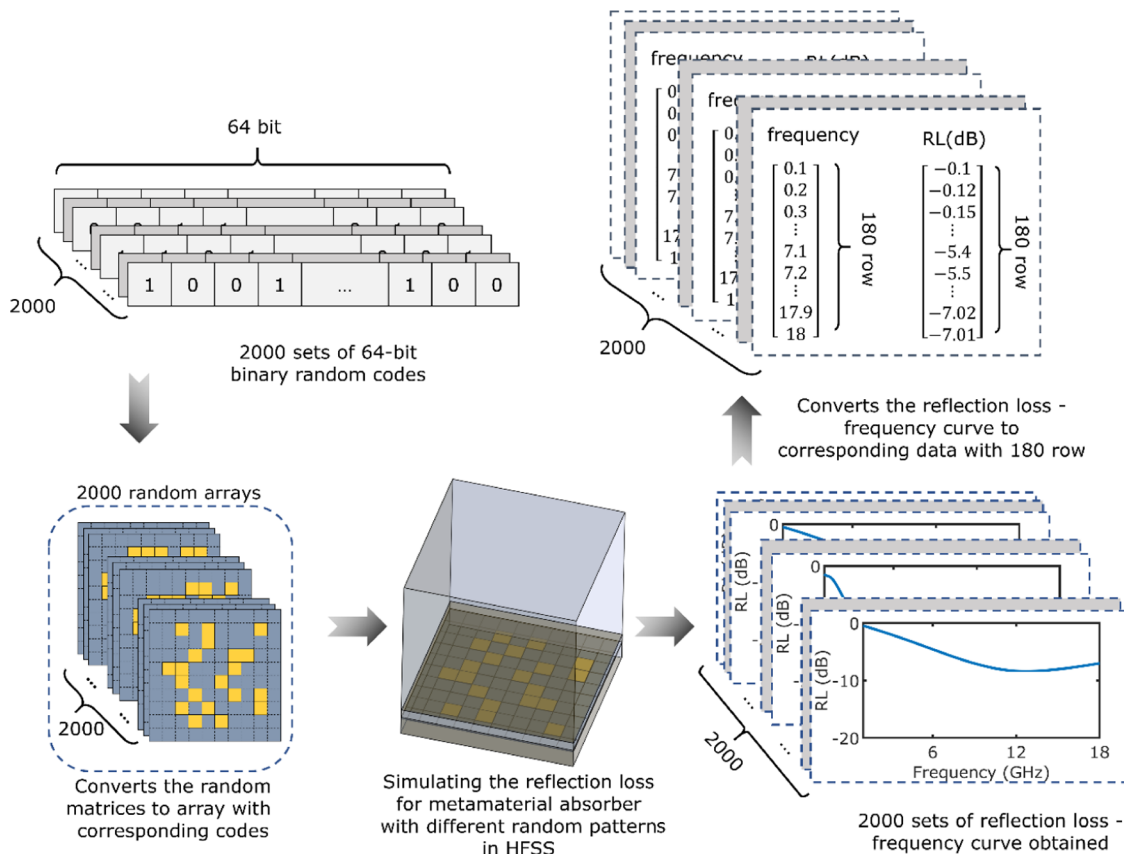


Figure 4. Process of collecting big data required for neural network training.

behavior characteristics of animal neural networks.³³ This type of network depends on the complexity of the system and achieves the purpose of processing information by adjusting the interconnected relations among a large number of nodes. It has been proven that a neural network with a hidden layer can approximate any function. Obviously, a well-trained neural network can be regarded as a function connecting the structure and absorption performance. Such a network can replace HFSS and provide fast solutions. To train a workable neural network, a large amount of data and a reasonable neural network structure are required.

For the desired data, we first randomly generated 2000 sets of random 64-bit binary codes, which, correspondingly, represent 2000 sets of different array patterns. By calling HFSS, we obtained the corresponding absorption performance data, as shown in Figure 4. The obtained absorption performance is frequency-dependent. To fit the absorption performance at different frequencies through the neural network, the 2000 sets of data are reorganized, as shown in Figure 5. The exported absorption performance in the range from 0.1 to 18 GHz was divided into 180 frequency points. The 2000 sets of data can be reorganized to 360 000 sets, which will be used as input values for training samples of the neural network. Similarly, the corresponding 360 000 sets of absorption performance points were used as the output values of the training neural network.

In this work, the back propagation (BP) neural network was chosen. As shown in Figure 5, our neural network has three layers, including an input layer, an intermediate layer, and an output layer. The input layer of the neural network has a total of 65 input units, which consists of 64 bits corresponding to

the metasurface structure and 1 bit to the frequency. The middle layer was set to 75 units. The output layer is one unit corresponding to the absorption performance for a certain frequency. We used 90% of the 360 000 samples for training and 10% for verification and finally obtained a trained neural network (the performance of the neural network is shown in Figure S2). We randomly generated different binary codes for verification, and the curve of reflection loss in the frequency obtained through the neural network was found to be in good agreement with the results of HFSS, as shown in Figures S3 and S4. Using the trained neural network, the calculation of the absorption performance for one pattern takes 0.06 s.

5. GENETIC ALGORITHM COMBINED WITH A NEURAL NETWORK

Accurate results can be obtained in a very short time using the neural network. Thus, the neural network can be used in the genetic algorithm to avoid repeated calls of HFSS to save time. The solution process of the genetic algorithm combined with the neural network is shown in Figure 6.

In this process, the object to be optimized is still the geometric structure of the array, that is, the codes of the metasurface. Hence, the length of the randomly generated individual chromosomes is 64 bits. As the input value of the trained neural network needs to include both the array code and the specified frequency to calculate the results at different frequencies, the structure codes and frequencies should be combined. As the aim is to obtain the widest bandwidth, the number of frequency points with a reflection loss value less than -10 dB was set as the fitness criteria. Based on the calculated fitness, the metasurface codes are selected, cross-

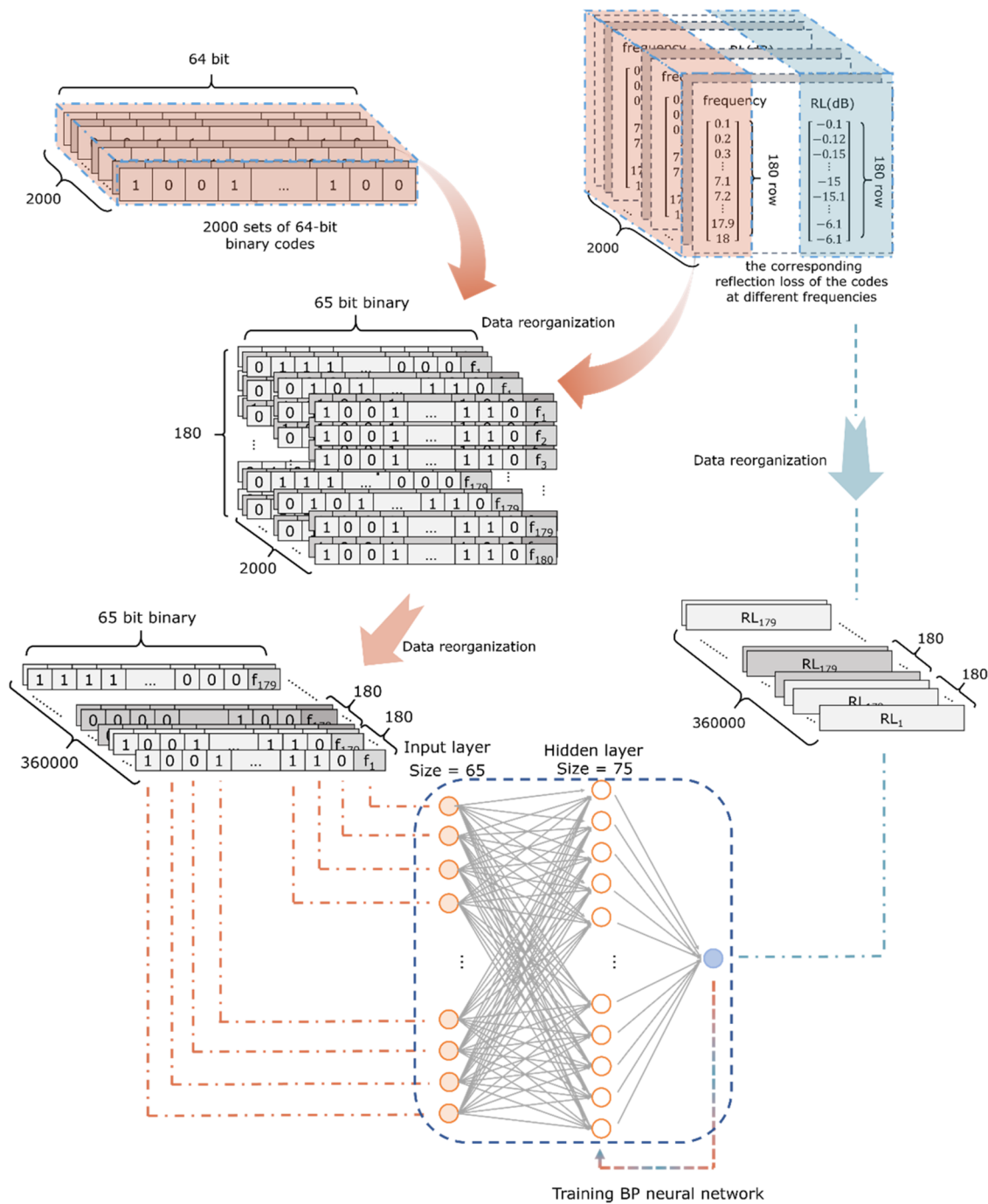


Figure 5. Schematic of neural network training.

recombined, and mutated to generate new individuals. These individuals are inserted back into the population consisting of their parents, and the above calculation process is repeated to obtain the optimal metasurface.

Due to the inclusion of the neural network, the whole genetic algorithm takes a very short time to find the optimal metasurface. It only takes 1 day to calculate the maximum genetic algebra of 100 with population N being 10 000. It took only 2 weeks to obtain the required training data and to train the neural network. If the training data are prepared with multiple computers at once, the time consumption can be reduced exponentially.

6. EXPERIMENT AND RESULTS

A double-layer magnetic medium was selected as the substrate, as shown in Figure S1a. Substrate A and substrate B are carbonyl iron-polyurethane compound with a volume fraction of 20 and 45%, respectively. They were prepared by tape casting.³⁴ The scanning electron microscopy images, electromagnetic parameters, and the reflection loss curve are shown in Figure S1. The metasurface is sandwiched between two layers to expand the absorption bandwidth, the schematic of which is shown in Figure 1b. The optimal metasurface pattern is obtained according to “Auto-BED”, as shown in Figure 7a. Using the printed circuit board method,³⁵ the metasurface was prepared as shown in Figure 7b. It was sandwiched between

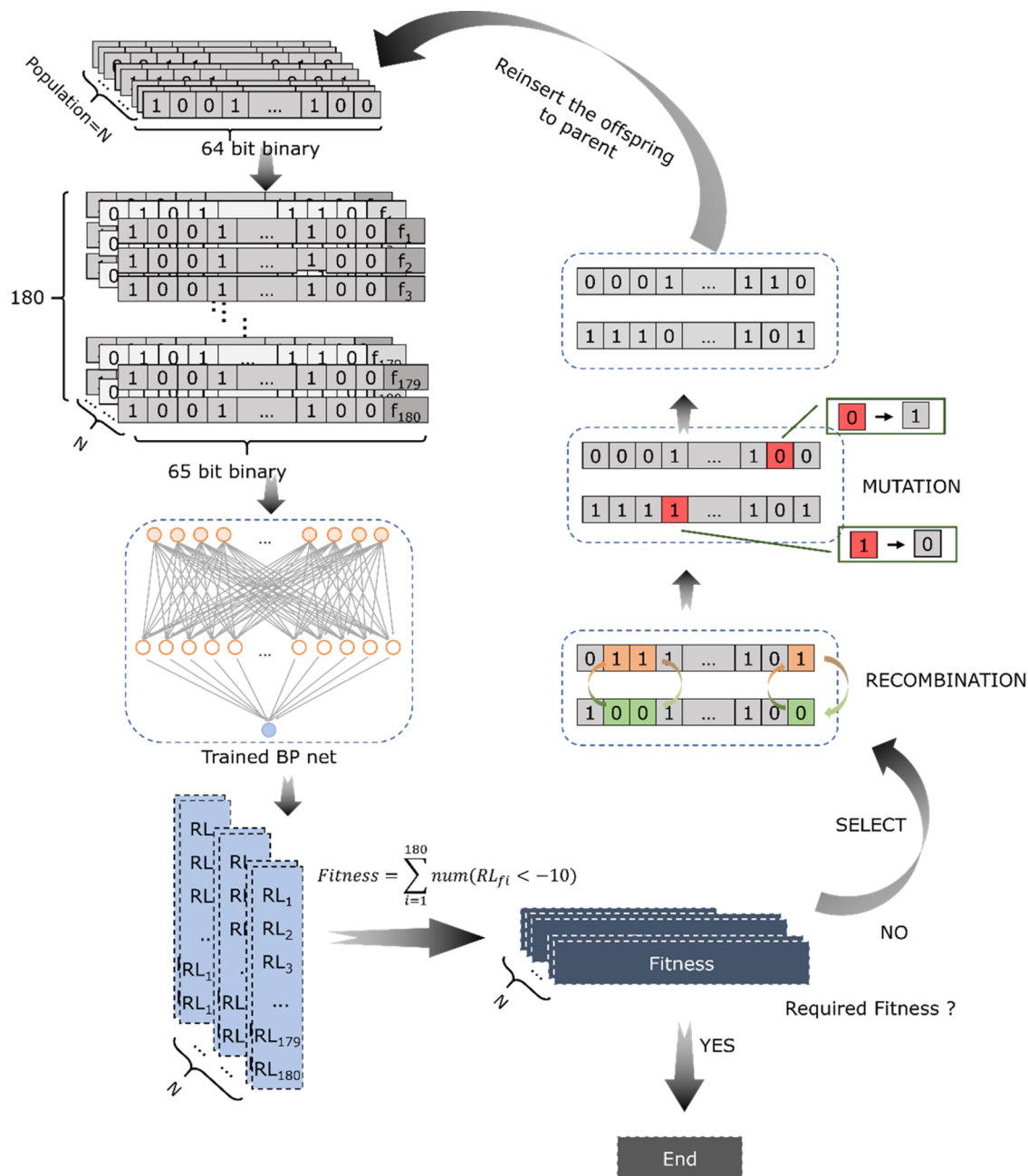


Figure 6. Flow chart of the algorithm to calculate the optimal metasurface using the genetic algorithm combined with a neural network.

the double-layer substrate, and the absorption performance of the metamaterial absorber was tested by the arch method. The test results (Figure 7d) show that the absorption bandwidth of the entire absorber has been extended to 13.5 GHz covering from 4.5 to 18 GHz. Compared with the previously presented different types of absorbers reported in the literature, the absorber designed by our method is not only thinner but also has a very wider absorption bandwidth, as observed from Table 1.

7. CONCLUSIONS

In this study, the automatic generation of metasurface array patterns was realized by controlling the metasurface codes. A back propagation neural network is used to calculate the absorption performance of various array encodings. Finally, a genetic algorithm is used to rapidly select the best-matched

metasurface design. The automated design of the broadband metasurfaces is realized by the combined operation of these three methods. This method is universal and can be used for different substrate materials. At the same time, the generated metasurface can be regarded as the best matched for the substrates in terms of the application bandwidth. For the experiments, we prepared a double-layer substrate with a bandwidth of 4.5 GHz. The metasurface generated by this method can increase this value to 13.5 GHz.

Although the strategy fills a gap in the field of metasurface design, there is still much space to progress. (1) There are limitations for the pattern design scheme in this article, for which we cannot completely approximate any potential structure. Only when the mesh network number of the unit pattern is greatly increased, it is possible to obtain the global optimal solution in the true sense of the word. But it also

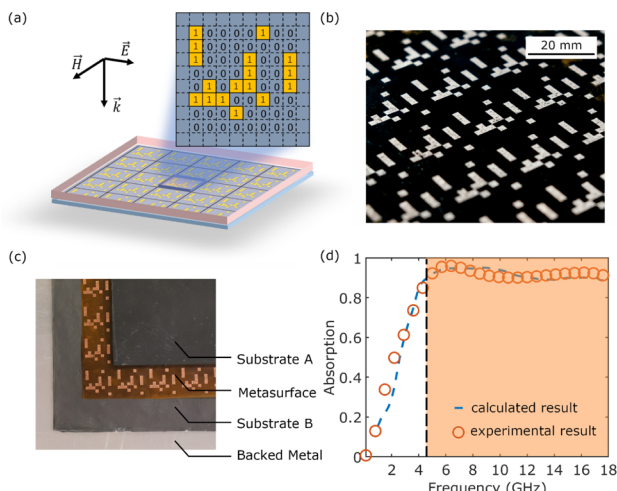


Figure 7. (a) Schematic of the obtained metasurface. (b) Image of the prepared metasurface array. (c) Image of the prepared metamaterial absorber. (d) Absorption performance of the metamaterial absorber.

Table 1. Comparison among the Different Broad-Band Absorbers

reference	type of absorber	thickness (mm)	-10 dB bandwidth (GHz)
36	conventional absorbing coating (single layer)	2.45	3.44 (8.12–11.56)
37	conventional absorbing coating (multilayer)	1.8	3.948 (9.056–13)
38	pyramid structure absorber	13.5	15 (3.5–18.5)
39	foam absorber	40	12.8 (4.7–5.4, 5.9–18)
40	metamaterial absorber (single-layer substrate)	3.4	5.8 (7–12.8)
41	metamaterial absorber (single-layer substrate)	2	8.79 (7.06–16.85)
42	metamaterial absorber (multilayer substrate)	3.65	12.63 (8.37–21)
43	metamaterial absorber (multilayer substrate)	4.6	13.26 (4.96–18.22)
this work	metamaterial absorber (multilayer substrate)	2.5	13.5 (4.5–18)

means that more training data are required to ensure the accuracy of the neural network training, which is a big challenge. (2) Many parameters with the ability affecting the performance were not taken into consideration. Adding more variable parameters may provide the potential for getting a better absorption performance. The material chosen for the metasurface may be a potential factor. Apart from metal materials with high conductivity (Cu, Ag, Au, and Al have been investigated, see the [Supporting Information](#)), ferrite materials or magnetic materials may be an interesting choice. (3) Except for the abovementioned issue, the absorption performance for different polarization and incident angles cannot be predicted by our model. We investigated the RL variation with the change of the polarization mode and the incident angle (see the [Supporting Information](#)). It is sensitive to different polarization and incident angle. Making the structure symmetrical may a good idea to solve the problem, or recollecting the data and training a new neural network may provide many more possibilities to solve all mentioned problems.

ASSOCIATED CONTENT

SI Supporting Information

The Supporting Information is available free of charge at <https://pubs.acs.org/doi/10.1021/acsami.0c21984>.

The schematic of the double-layer substrate (Figure S1); the performance of the BP neural network (Figure S2); the comparison of results from HFSS and the trained BP neural network (Figure S3); and the comparison of RL for the metasurface in different metal materials (Figure S7) ([PDF](#))

AUTHOR INFORMATION

Corresponding Author

Tao Wang – Key Laboratory for Magnetism and Magnetic Materials, Ministry of Education and Key Laboratory of Special Function Materials and Structure Design, Ministry of Education, Lanzhou University, Lanzhou 730000, People's Republic of China; Email: wtao@lzu.edu.cn

Authors

Junming Zhang – Key Laboratory for Magnetism and Magnetic Materials, Ministry of Education, Lanzhou University, Lanzhou 730000, People's Republic of China; orcid.org/0000-0003-2731-7289

Guowu Wang – Key Laboratory for Magnetism and Magnetic Materials, Ministry of Education, Lanzhou University, Lanzhou 730000, People's Republic of China

Fashen Li – Key Laboratory for Magnetism and Magnetic Materials, Ministry of Education, Lanzhou University, Lanzhou 730000, People's Republic of China

Complete contact information is available at: <https://pubs.acs.org/10.1021/acsami.0c21984>

Funding

This work was supported by the National Natural Science Foundation of China (no. 11574122) and the Joint Fund of Equipment Pre-Research and Ministry of Education (no. 6141A02033242).

Notes

The authors declare no competing financial interest.

REFERENCES

- (1) Landy, N. I.; Sajuyigbe, S.; Mock, J. J.; Smith, D. R.; Padilla, W. J. Perfect Metamaterial Absorber. *Phys. Rev. Lett.* **2008**, *100*, No. 207402.
- (2) He, M.; Zhou, Y.; Huang, T.; Nie, S.; Wang, Y.; Xu, Z.; Huo, Y.; Xu, R.; Chen, X.; Peng, H. Flower-like CoS hierarchitectures@ polyaniline organic-inorganic heterostructured composites: preparation and enhanced microwave absorption performance. *Compos. Sci. Technol.* **2020**, *200*, No. 108403.
- (3) Lei, L.; Yao, Z.; Zhou, J.; Wei, B.; Fan, H. 3D printing of carbon black/polypropylene composites with excellent microwave absorption performance. *Compos. Sci. Technol.* **2020**, *200*, No. 108479.
- (4) Wang, T.; Han, R.; Tan, G.; Wei, J.; Qiao, L.; Li, F. Reflection loss mechanism of single layer absorber for flake-shaped carbonyl-iron particle composite. *J. Appl. Phys.* **2012**, *112*, No. 104903.
- (5) Yang, J.; Pang, Y.; Wang, J.; Sui, S.; Jiang, W.; Zhang, J.; Qu, S. Achieving broadband RCS reduction using carbon fiber connected composite via scattering mechanism. *Compos. Sci. Technol.* **2020**, *200*, No. 108410.
- (6) Pai, A. R.; Binumol, T.; Gopakumar, D. A.; Pasquini, D.; Thomas, S.; Kalarikkal, N.; Thomas, S. Ultra-Fast Heat Dissipating Aerogels Derived from Polyaniline Anchored Cellulose Nanofibers as

- Sustainable Microwave Absorbers. *Carbohyd. Polym.* **2020**, *246*, No. 116663.
- (7) Pang, Y.; Li, Y.; Qu, B.; Yan, M.; Wang, J.; Qu, S.; Xu, Z. Wideband RCS Reduction Metasurface with a Transmission Window. *IEEE Trans. Antennas Propag.* **2020**, *68*, 7079–7087.
- (8) Kuchi, R.; Nguyen, H. M.; Dongquoc, V.; Van, P. C.; Ahn, H.; Viet, D. D.; Kim, D.; Kim, D.; Jeong, J.-R. Optimization of FeNi/SWCNT composites by a simple co-arc discharge process to improve microwave absorption performance. *J. Alloys Compd.* **2021**, *852*, No. 156712.
- (9) Zhang, Y.; Si, H.; Liu, S.; Jiang, Z.; Gong, C. Facile synthesis of BN/Ni nanocomposites for effective regulation of microwave absorption performance. *J. Alloys Compd.* **2021**, *850*, No. 156680.
- (10) Abdalla, I.; Salim, A.; Zhu, M.; Yu, J.; Li, Z.; Ding, B. Light and Flexible Composite Nanofibrous Membranes for High-Efficiency Electromagnetic Absorption in a Broad Frequency. *ACS Appl. Mater. Interfaces* **2018**, *10*, 44561–44569.
- (11) Ma, J.; Liu, W.; Liang, X.; Quan, B.; Cheng, Y.; Ji, G.; Meng, W. Nanoporous TiO₂/C composites synthesized from directly pyrolysis of a Ti-based MOFs MIL-125(Ti) for efficient microwave absorption. *J. Alloys Compd.* **2017**, *728*, 138–144.
- (12) He, F.; Zhao, Y.; Si, K.; Zha, D.; Li, R.; Dong, J.; Bie, S.; Jiang, J. Multisection step-impedance modeling and analysis of broadband microwave honeycomb absorbing structures. *J. Phys. D: Appl. Phys.* **2021**, *54*, No. 015501.
- (13) Yang, Z.; Luo, F.; Zhou, W.; Zhu, D.; Huang, Z. Design of a broadband electromagnetic absorbers based on TiO₂/Al₂O₃ ceramic coatings with metamaterial surfaces. *J. Alloys Compd.* **2016**, *687*, 384–388.
- (14) Zhao, B.; Huang, C.; Yang, J.; Song, J.; Guan, C.; Luo, X. Broadband Polarization-insensitive Tunable Absorber Using Active Frequency Selective Surface. *IEEE Antennas Wireless Propag. Lett.* **2020**, *19*, 982–986.
- (15) Duan, B.; Zhang, J.; Wang, P.; Wang, G.; He, D.; Qiao, L.; Wang, T. Design and preparation of an ultrathin broadband metamaterial absorber with a magnetic substrate based on genetic algorithm. *J. Magn. Magn. Mater.* **2020**, *501*, No. 166439.
- (16) Agarwal, S.; Prajapati, Y. K.; Singh, V.; Saini, J. P. Polarization independent broadband metamaterial absorber based on tapered helical structure. *Opt. Commun.* **2015**, *356*, 565–570.
- (17) Long, Y.; Deng, H.; Xu, H.; Shen, L.; Guo, W.; Liu, C.; Huang, W.; Peng, W.; Li, L.; Lin, H.; Guo, C. Magnetic coupling metasurface for achieving broad-band and broad-angular absorption in the MoS₂ monolayer. *Opt. Mater. Express* **2017**, *7*, No. 100.
- (18) Su, P.; Zhao, Y.; Jia, S.; Shi, W.; Wang, H. An Ultra-wideband and Polarization-independent Metasurface for RCS Reduction. *Scientific Reports* **2016**, *6*, No. 20387.
- (19) Fan, Y.; Wang, J.; Li, Y.; Pang, Y.; Zheng, L.; Xiang, J.; Zhang, J.; Qu, S. Ultra-thin and -broadband microwave magnetic absorber enhanced by phase gradient metasurface incorporation. *J. Phys. D: Appl. Phys.* **2018**, *51*, No. 215001.
- (20) Xu, H.-X.; Zhang, L.; Kim, Y.; Wang, G.-M.; Zhang, X.-K.; Sun, Y.; Ling, X.; Liu, H.; Chen, Z.; Qiu, C.-W. Wavenumber-Splitting Metasurfaces Achieve Multichannel Diffusive Invisibility. *Adv. Opt. Mater.* **2018**, *6*, No. 1800010.
- (21) Cui, T. J.; Qi, M. Q.; Wan, X.; Zhao, J.; Cheng, Q. Coding metamaterials, digital metamaterials and programmable metamaterials. *Light: Sci. Appl.* **2014**, *3*, No. e218.
- (22) Cai, H.; Sun, Y.; Wang, X.; Zhan, S. Design of an ultra-broadband near-perfect bilayer grating metamaterial absorber based on genetic algorithm. *Opt. Express* **2020**, *28*, 15347–15359.
- (23) Huang, Y.; Fan, Q.; Chen, J.; Li, L.; Chen, M.; Tang, L.; Fang, D. Optimization of flexible multilayered metastructure fabricated by dielectric-magnetic nano lossy composites with broadband microwave absorption. *Compos. Sci. Technol.* **2020**, *191*, No. 108066.
- (24) Qiu, T.; Shi, X.; Wang, J.; Li, Y.; Qu, S.; Cheng, Q.; Cui, T.; Sui, S. Deep Learning: A Rapid and Efficient Route to Automatic Metasurface Design. *Adv. Sci.* **2019**, *6*, No. 1900128.
- (25) Aslan, E.; Aslan, E.; Turkmen, M.; Saracoglu, O. G. Experimental and numerical characterization of a mid-infrared plasmonic perfect absorber for dual-band enhanced vibrational spectroscopy. *Opt. Mater.* **2017**, *73*, 213–222.
- (26) Nguyen, T. T.; Lim, S. Bandwidth-enhanced and Wide-angle-of-incidence Metamaterial Absorber using a Hybrid Unit Cell. *Sci. Rep.* **2017**, *7*, No. 14814.
- (27) Wu, B.; Liu, Z.; Du, G.; Chen, Q.; Liu, X.; Fu, G.; Liu, G. Polarization and angle insensitive ultra-broadband mid-infrared perfect absorber. *Phys. Lett. A* **2020**, *384*, No. 126288.
- (28) Gao, L.-H.; Cheng, Q.; Yang, J.; Ma, S.-J.; Zhao, J.; Liu, S.; Chen, H.-B.; He, Q.; Jiang, W.-X.; Ma, H.-F.; Wen, Q.-Y.; Liang, L.-J.; Jin, B.-B.; Liu, W.-W.; Zhou, L.; Yao, J.-Q.; Wu, P.-H.; Cui, T.-J. Broadband diffusion of terahertz waves by multi-bit coding metasurfaces. *Light: Sci. Appl.* **2015**, *4*, No. e324.
- (29) Wu, L. W.; Ma, H. F.; Wu, R. Y.; Xiao, Q.; Gou, Y.; Wang, M.; Wang, Z. X.; Bao, L.; Wang, H. L.; Qing, Y. M.; Cui, T. J. Transmission-Reflection Controls and Polarization Controls of Electromagnetic Holograms by a Reconfigurable Anisotropic Digital Coding Metasurface. *Adv. Opt. Mater.* **2020**, *8*, No. 2001065.
- (30) Zhang, J.; Zhang, H.; Yang, W.; Chen, K.; Wei, X.; Feng, Y.; Jin, R.; Zhu, W. Dynamic Scattering Steering with Graphene-Based Coding Metamirror. *Adv. Opt. Mater.* **2020**, *8*, No. 2000683.
- (31) Patchaikani, S.; Kuwahara, Y. GA optimization of transparent MIMO antenna for smartphone. *IEICE Electron. Express* **2013**, *10*, No. 20130288.
- (32) Haupt, R. L. Using MATLAB to control commercial computational electromagnetics software. *Appl. Comput. Electromagn. Soc. J.* **2008**, *23*, 98–103.
- (33) Abdullah, S.; Pradhan, R. C.; Pradhan, D.; Mishra, S. Modeling and optimization of pectinase-assisted low-temperature extraction of cashew apple juice using artificial neural network coupled with genetic algorithm. *Food Chem.* **2021**, *339*, No. 127862.
- (34) Fang, Z.; Lu, C.; Lu, Y.; Ma, D.; Wei, L.; Li, P.; Ni, Y.; Tao, S.; Xu, Z. Radiation heat transfer enhanced absorber for high temperature solar-thermal applications. *Ceram. Int.* **2016**, *42*, 10531–10536.
- (35) Zuo, P.; Li, T.; Wang, M.; Zheng, H.; Li, E.-P. Miniaturized Polarization Insensitive Metamaterial Absorber Applied on EMI Suppression. *IEEE Access* **2020**, *8*, 6583–6590.
- (36) Huang, W.; Tong, Z.; Li, W.; Ma, M.; Bi, Y.; Liao, Z.; Wang, R.; Ma, Y. Fabrication of flower-like ZnFe₂O₄@SiO₂@C@NiO nano-chains/reduced graphene oxides as a high-performance microwave absorber. *J. Alloys Compd.* **2020**, *849*, No. 156658.
- (37) Padhy, S.; De, A.; Debata, R. R.; Meena, R. S. Design, Characterization, and Optimization of a Multilayer U-type Hexaferrite-Based Broadband Microwave Absorber. *IEEE Trans. Electromagn. Compat.* **2018**, *60*, 1734–1742.
- (38) Van Hoang, T. Q.; Loiseaux, B. In *Ultra-Broadband Multilayer Microwave Absorber by Multimaterial 3D Printing*, 2020 14th European Conference on Antennas and Propagation; IEEE, 2020.
- (39) Wu, F.; Li, Y.; Lan, X.; Huang, P.; Chong, Y.; Luo, H.; Shen, B.; Zheng, W. Large-scale fabrication of lightweight, tough polypropylene/carbon black composite foams as broadband microwave absorbers. *Compos. Commun.* **2020**, *20*, No. 100358.
- (40) Nguyen, T. T.; Lim, S. Angle-and polarization-insensitive broadband metamaterial absorber using resistive fan-shaped resonators. *Appl. Phys. Lett.* **2018**, *112*, No. 021605.
- (41) Gao, H.; Wang, J.; Xu, B.; Li, Z.; Suo, Q. Broadband metamaterial absorber based on magnetic substrate and resistance rings. *Mater. Res. Express* **2019**, *6*, No. 045803.
- (42) Xiong, H.; Hong, J.-S.; Luo, C.-M.; Zhong, L.-L. An ultrathin and broadband metamaterial absorber using multi-layer structures. *J. Appl. Phys.* **2013**, *114*, No. 064109.
- (43) Ghosh, S.; Bhattacharyya, S.; Srivastava, K. V. Design, characterisation and fabrication of a broadband polarisation-insensitive multi-layer circuit analogue absorber. *IET Microwaves Antennas Propag.* **2016**, *10*, 850–855.